Since January 2020 Elsevier has created a COVID-19 resource centre with free information in English and Mandarin on the novel coronavirus COVID-19. The COVID-19 resource centre is hosted on Elsevier Connect, the company's public news and information website.

Computers in Biology and Medicine 137 (2021) 104818

Contents lists available at ScienceDirect

Computers in Biology and Medicine

journal homepage: www.elsevier.com/locate/compbiomed

In silico study of some selective phytochemicals against a hypothetical SARS-CoV-2 spike RBD using molecular docking tools

Anish Nag [a], Subhabrata Paul [b], Ritesh Banerjee [c], Rita Kundu [d,*]

[a] Department of Life Sciences, CHRIST (Deemed to Be University), Bangalore 560029, India
[b] School of Biotechnology, Presidency University, Canal Bank Rd, DG Block, Action Area 1D, New Town, West Bengal 700156, India
[c] School of Biological and Environmental Sciences, Shoolini University, Solan, Himachal Pradesh, 173229, India
[d] Department of Botany, University of Calcutta, 35, Ballygunge Circular Road, Kolkata 700019, India

ARTICLE INFO

Keywords:
COVID-19
Coronavirus
Spike-RBD
ACE2
Mutated spike
In silico study

ABSTRACT

Background: This world is currently witnessing a pandemic outbreak of 'COVID-19' caused by a positive-strand RNA virus 'SARS-CoV-2'. Millions have succumbed globally to the disease, and the numbers are increasing day by day. The viral genome enters into the human host through interaction between the spike protein (S) and host angiotensin-converting enzyme-2 (ACE2) proteins. S is the common target for most recently rolled-out vaccines across regions. A recent surge in single/multiple mutations in S region is of great concern as it may escape vaccine induced immunity. So far, the treatment regime with repurposed drugs has not been too successful.

Hypothesis: Natural compounds are capable of targeting mutated spike protein by binding to its active site and destabilizing the spike-host ACE2 interaction.

Materials and methods: A hypothetical mutated spike protein was constructed by incorporating twelve different mutations from twelve geographical locations simultaneously into the receptor-binding domain (RBD) and docked with ACE2 and seven phytochemicals namely allicin, capsaicin, cinnamaldehyde, curcumin, gingerol, piperine and zingeberene. Molecular Dynamic (MD) simulation and Principal Component Analysis (PCA) were finally used for validation of the docking results.

Result: The docking results showed that curcumin and piperine were most potent to bind ACE2, mutated spike, and mutated spike-ACE2 complex, thereby restricting viral entry. ADME analysis also proved their drug candidature. The docking complexes were found to be stable by MD simulation.

Conclusion: This result provides a significant insight about the phytochemicals' role, namely curcumin and piperine, as the potential therapeutic entities against mutated spike protein of SARS-CoV-2.

1. Introduction

The 21st century has witnessed its first pandemic, COVID-19, caused by a novel coronavirus SARS-CoV-2. More than 100 million cases were reported worldwide, with 4 million deaths [1] and still counting. The SARS-CoV-2 disease is similar to the previous corona virus outbreaks of SARS-CoV and MERS-CoV that occurred in 2002 and 2012 respectively. SARS-CoV-2, a member of β-coronavirus, like SARS-CoV and MERS-CoV, also infects the lower respiratory tract of humans. It belongs to the genus *betacoronavirus* of the order *Nidovirales*, family *Coronaviridae*, and subfamily *Coronavirinae*. It is an enveloped virus with a positive-sense single-stranded RNA. The non-segmented viral genome is about 30 kb in size [2], which codes for several non-structural and structural proteins, including surface, nucleocapsid, membrane and envelope glycoproteins (S, N, M and E). The genome is encapsulated by a spherical envelope with *trans*-membrane glycoproteins protruding from the surface which trimerizes to form the spike proteins (S). The S protein is composed of two subunits, S1, and S2. The receptor-binding domain (RBD), present in S1subunit is essential for viral entry into the host body and is mediated by binding with human angiotensin-converting enzyme-2 (ACE2) receptors. According to Zhou et al. [3] it is the most variable part of the SARS-CoV-2 genome, making it different from other SARS-CoV genomes. L455, F486, Q493, S494, N501 and Y505 are the unique amino acids present in the RBD domain of SARS-CoV-2, which are different

* Corresponding author.
E-mail address: rkbot@caluniv.ac.in (R. Kundu).

https://doi.org/10.1016/j.compbiomed.2021.104818
Received 26 April 2021; Received in revised form 26 August 2021; Accepted 26 August 2021
Available online 28 August 2021

from the amino acid sequence present in SARS-CoV RBD [4]. SARS-CoV-2 RBD also shows a high binding affinity for cat, ferret and pangolin ACE2 receptors, this property is attributed for its cross-species infecting capabilities [5]. Available reports showed that, 90.55 and 91.02% sequence similarities exist between Pangolin-CoV with Bat-CoV RaTG13 and SARS-CoV-2, respectively [6]. The junction of two spike subunits S1 and S2, houses a polybasic furin cleavage site (RRAR) in the SARS-CoV-2 genome [7], which can be cleaved by proteases (Transmembrane Protease Serine2, TMPRSS2) affecting viral infectivity in different hosts [8]. This site's cleavage is essential for the fusion of the host cell membrane with that of the virus, and is considered critical for entry into the host body. The addition of a proline residue makes the cleavage site PRRAR and thereby, O-linked glycans are added to S673, T678 and S686 residues, flanking the cleavage site. However, the function of these O-linked glycans is not known specifically (as these O-linked glycans are reported to have multiple roles, from assisting viral entry to evading a host's antibody), but is unique to SARS-CoV-2. "Mucin like domains" can be formed by them to protect SARS-CoV-2 S protein epitopes [9]. As drug and vaccine development against COVID-19 is a lengthy procedure, physicians are trying to stress more on prevention than cure for treating the disease. To give some relief to the patients, mostly repurposed drugs against COVID-19 are being used, but none of them showed cent percent efficacy. Though several vaccines have been developed by the untiring efforts of scientists worldwide, none of them is time tested and cannot guarantee a foolproof protection. At the same time, it is not possible to predict the stability of the neutralizing antibodies, therefore, it is also not known for how long the vaccine-induced immunity against COVID-19 will persist. Due to the error-prone nature of RNA dependent RNA polymerases (RdRp), which is a characteristic feature of RNA viruses, ample natural mutations occur, producing multiple subtypes of SARS-CoV-2. A study of 3686 probable future mutations in the S protein binding domain was predicted with increased infectivity [10]. Therefore, the consistent emergence of several mutated strains becomes a persistent threat [11]. The present study targeted twelve such mutations of S protein, based on its geographical frequency distribution obtained from the GISAID database. All the mutations are incorporated together in the S protein, considering a hypothetical condition when the virus may simultaneously encompass all such changes. The emergence of several double/multiple mutants [12,13] with more infectivity than that of single mutations [14], led us to design this study with a hypothetical spike model with several mutations at a time. Recently a new variant (known as B.1.617 or delta variant) with multiple mutations – the E484Q, L452R and T478K was detected in India [15] and other parts of the world. This variant showed higher transmissibility and infectivity, as multiple mutations in the spike RBD increases its affinity to bind ACE2 [16,17]. Several mutations also made SARS-CoV-2 more resistant to antibodies [18,19].

The high affinity between SARS-CoV-2 spike RBD and human ACE2 protein enables viral entry into the host cell. The furin mediated pre-activation of S protein makes it less dependent on the host protease for its entry into host cells. This unique feature and hidden S protein RBD make SARS-CoV-2 efficient in evading host cell immunity and contributes to its widespread distribution. Several intervention strategies are already being developed based on viral entry; and such interventions should be continued. For example, anti-malarial drugs like chloroquine, and hydroxy-chloroquine were found to inhibit the endocytic pathway, restricting S protein cleavage at the ACE2 binding site [20] are presently repurposed to treat COVID-19. Chloroquine can act against SARS-CoV-2 through multiple pathways. Either, it can inhibit the endocytic pathway by increasing the endosomal pH, or it can inhibit the binding with SARS-CoV-2 RBD by altering the glycosylation of ACE2 receptor [21,22]. However, these compounds also have certain adversities, such as lesser solubility in water and may cause ocular and renal toxicity. Hence, finding new safer compounds targeting S-ACE2 binding and blocking ACE2 altogether maybe the best options to prevent viral entry.

Several phytochemicals are already being tested for their anti-SARS-CoV-2 activity by *in silico* approach. Researchers are looking for new lead phytochemicals all over the world, which will strongly inhibit the entry and pathogenicity of SARS-CoV-2 in host cells. S protein, ACE2 protein and SARS-CoV-2 protease are their prime targets. Hesperidin from *Citrus* sp. was found to bind with the spike-ACE2 complex [23]. Galangin, curcumin and brazilin were found to target both the RBD of spike and protease proteins [24]. In this present study, seven phytochemicals, allicin, capsaicin, cinnamaldehyde, curcumin, gingerol, piperine and zingiberene were tested for their ACE2 blocking potential and targeting spike-ACE2 binding. Curcumin is a well-known antiviral compound exhibiting activity against several viruses, like Zika, HSV, HIV, HPV etc. [25,26] and was previously reported as an anti-ACE2, anti-spike &anti-protease agent [27–29]. Piperine, a major alkaloid from black pepper, showed substantial anti-inflammatory properties by down-regulating pro-inflammatory cytokine production [30]. As continuous reports of mutated strains are coming in, it was observed that the mutations accumulated in the RBD domain of S protein are most critical, as this domain plays a major role in pathogenicity. In this study, seven phytochemicals were tested for their ACE2 blocking potential and targeting destabilization of spike-ACE2 binding. At the same time, the present study also aimed to explore the efficacy of these selected phytochemicals for their binding affinity with the mutated spike protein and ACE2 by *in silico* analysis. Here, we have tried to explore the efficacy of the phytochemicals against a hypothetical RBD, in which twelve mutations from different geographical locations are clubbed together in the same spike protein. This is the uniqueness of this study, which has so far, not been reported.

2. Materials and method

2.1. Sequence and structure

The three-dimensional structure of the SARS-CoV-2 Spike (S) protein hACE2 receptor-binding domain [RBD] (PDB id 6M0J, Chain A and E, X-Ray Diffraction, Resolution 2.45 Å) was downloaded from RCSB PDB (https://www.rcsb.org/). This model was selected based on a high-resolution crystal structure (2.45 Å) determined by X-ray diffraction methodology. Spike protein receptor-binding domain (Chain E) and ACE2 protein (Chain A) were separated from the complex using UCSF Chimera software. The primary amino acid sequence (hCoV-19/Wuhan/WIV04/2019, WIV04) of the native spike protein receptor-binding domain (RBD)- "TNLCPFGEVFNATRFASVYAWNRKRISNCVADYSVLYNSASFSTFKCYGVSPTKLNDLCFTNVYADSFVIRGDEVRQIAPGQTGKIADYNYKLPDDFTGCVIAWNSNNLDSKVGGNYNYLYRLFRKSNLKPFERDISTEIYQAGSTPCNGVEGFNCYFPLQSYGFQPTNGVGYQPYRVVVLSFELLHAPATVCGPKKSTNLVKNKCVNF" (position 333 to 541) was confirmed from GISAID (https://www.gisaid.org).

Further twelve major mutations of the S protein namely V382L (geological frequency179, hCoV-19/Gambia/NPHL-2554/2020), P384L (geological frequency 104, hCoV-19/England/EXET-137CED/2020), K417 N (geological frequency 218,hCoV-19/Austria/CeMM1952/2020), N439K (geological frequency 5725, hCoV-19/England/CAMB-1BD906/2020), Y453F (geological frequency 968, hCoV-19/Netherlands/NB-EMC-267/2020), S477 N (geological frequency 16914, hCoV-19/Netherlands/NB-EMC-267/2020), T478I (geological frequency 205,hCoV-19/England/CAMB-81140/2020), E484K (geological frequency 310,hCoV-19/Austria/CeMM1952/2020), S494P (geological frequency 164, hCoV-19/England/CAMB-A9A757/2020), N501Y (geological frequency 4362, hCoV-19/England/205261952/2020) and A520S (geological frequency 452,hCoV-19/USA/WA-S137/2020) based on geological frequency distribution were selected from GSAID. These mutations were incorporated together into the 3D structure of spike protein ACE2 receptor-binding domain (6M0J.E) by using PyMOL 2.4 software [31] (The PyMOL Molecular Graphics System; http://www.pymol.org).

2.2. Selection and preparation of ligands

The three-dimensional structures of the phytochemicals, namely, allicin (CID 65036), capsaicin (CID 1548943), cinnamaldehyde (CID 637511), curcumin (CID 969516), gingerol (CID 442793), piperine (CID 638024) and zingiberene (CID 92776) and the control drugs chloroquine (CID 2719) & GR 127935 hydrochloride (CID 107780) were downloaded from PubChem database (https://pubchem.ncbi.nlm.nih.gov/) in .SDF format. Control drug chloroquine was selected based on its reported efficacy against the spike protein of SARS-CoV-2 [32,33] and human ACE2 proteins [34] respectively. Furthermore, we also included GR 127935 hydrochloride (CID 107780) as an additional control against hACE2 protein. Choudhary et al. [35] showed GR 127935 hydrochloride as a potential inhibitor against hACE2 protein in SARS-CoV-2 pathogenesis using *in silico* structure-based virtual screening approach. Structural optimization (energy minimization and protonation) and conversion in.PDB format were performed by Avogadro software before conducting the molecular docking analysis. For ligand energy optimization, a universal force field (UFF) algorithm was applied. UFF is capable of reproducing the most structural features across the periodic table. It can do transition state searches by calculating single point energies, frequencies, and geometric optimization. Finally, UFF cleans up manually drawn structures and calculates with chain, slab or bulk periodicity [36].

2.3. Evaluation of drug-like properties

SwissADME [37] predicts ADME (Absorption, Distribution, Metabolism, and Excretion) of the input compounds through multiple parameters such as pharmacokinetic properties, drug-like nature and medicinal chemistry etc. and also computes physiochemical descriptors. In this study, the canonical smile formats of eight compounds, including the control drug chloroquine, were uploaded to the SwissADME (http://www.swissadme.ch/) site to evaluate their pharmacological and drug-likeness potential. Evaluation of drug-likeness of the input ligands was done by Boiled-Egg graphical interface and by ADME parameters such as TPSA, iLOGP, ESOL Log S, Lipinski Violations, Leadlikeness and Bioavailability score [38].

2.4. Molecular docking between spike protein receptor-binding domain (S) and hACE2 protein

Molecular docking between native S, mutated S protein, and hACE2 proteins were performed by ClusPro 2.2 online server (https://cluspro.bu.edu/publications.php). ClusPro works by rotating ligands with 70,000 rotations, and 1000 rotations/translation combinations were selected based on the lowest score. Finally, best clusters were reported based on ligand positions with the closest "neighbours" within 9 Å [39]. Cluspro 2.0 was experimentally validated in the literature. Chance and his coworkers performed protein-protein docking with the actin-binding protein cofilin and monomeric actin. Further, it was validated experimentally by hydroxyl radical-mediated oxidative protein foot-printing [40,41]. Padhorny et al. [42] established the validity and accuracy of docking predictions in the protein docking experiment CAPRI (Critical Assessment of Predicted Interactions).

The protein-protein binding affinity between S and hACE2 proteins is an important criterion to understand the affinity of S protein to hACE2 due to mutations. The binding energy was expressed by binding affinity (in kcal mol^{-1}). The binding affinities (binding energy ΔG expressed in kcal mol^{-1}) between S (native and mutated) and hACE2 proteins were predicted by the PRODIGY web server (https://wenmr.science.uu.nl/prodigy/). PRODIGY (protein binding energy) is an open-source web server that produces binding energy between biological complexes and identifies biological interfaces from the crystallographic macromolecular structures [43].

2.5. Molecular docking between phytochemicals and proteins

Molecular docking analysis between phytochemicals and proteins was performed by DockThor web program (https://dockthor.lncc.br/v2/). It is a flexible open-source docking algorithm that utilizes in-house tools, namely MMFF Ligand and PdbThorBox, and contains topology files for the ligands. It uses partial charges from the MMFF94S53 force field for the protein inputs [44]. All docking results of phytochemicals were compared to the control drug chloroquine, and thereby the best phytochemicals were selected.

2.5.1. Phytochemicals and S proteins

Phytochemicals, namely allicin, capsaicin, cinnamaldehyde, curcumin, gingerol, piperine and zingiberene and the control drug chloroquine were docked with native S protein in the target binding mode (targeting interaction site between hACE2 and S) with the grid parameters center x/y/z = −39/36/8 and size x = 24/29/20.

2.5.2. Phytochemicals and hACE2 protein

Phytochemicals and the control drugs (chloroquine and GR 127935 hydrochloride) were docked with hACE2 protein in the target binding mode with the grid parameters center x/y/z = −42.25/12.621/-43.746 & size x/y/z = 31/21/28.

2.5.3. Phytochemicals and S-hACE2 complex

Phytochemicals, and the control drug chloroquine, were docked with native S-hACE2 and mutated S-hACE2 complexes in the target binding mode with the grid parameters center x/y/z = −42.25/12.621/-43.746 & size x/y/z = 33/21/28 and center x = −42.25/12.621/-43.746 & size x/y/z = 34/20/21, respectively.

2.6. Visualization and protein-ligand interaction analysis

UCSF Chimera 1.15 is an open-source program for the interactive visualization and analysis of molecular docked structures and creates high-quality images of the structured models [45]. BIOVIA Discovery Studio Visualizer (Dassault Systems) software was used to identify the interaction sites of protein-ligand contacts. In this work, the docking interaction, visualization and graphical rendering were performed by UCSF Chimera and BIOVIA Discovery Studio 2020.

2.7. Docking validation by molecular dynamic (MD) simulation

The molecular docking simulations of curcumin and piperine with S proteins (native and mutated spike proteins) were performed by using a GROMACS-2019.2 [46] based bio-molecular package provided by the Simlab, the University of Arkansas for Medical Sciences (UAMS), Little Rock, USA. The protein-ligand interactions were approximated by GROMOS96 43a1 force field [47], and ligand topology files were generated by PRODRG software [48]. A triclinic box was selected for each ligand-protein complex, filled with SPC water, and 0.15 M counter ions (Na+/Cl-) were added to neutralize the system with NVT/NPT ensemble temperature 300K & atmospheric pressure (1 bar). The temperature and the pressure were controlled by Parrinello-Danadio-Bussi thermostat [49] and Parrinello-Rahmanbarostat [50,51]. The resulting systems were energy minimised by 5000 steepest descent integrator. Each complex was simulated for 100 ns, and snapshots were saved for every 10 ns. Several parameters were evaluated for assessing the stability of protein-ligand complexes, namely Root Mean Square Deviation (RMSD), the radius of gyration (Rg), Solvent Accessible Surface Area (SASA), and h bonds.

2.8. Statistical analysis, heat map generationand molecular alignment

Principal Component Analysis (PCA) is a multivariate statistical analysis tool that transforms measured variables into principal

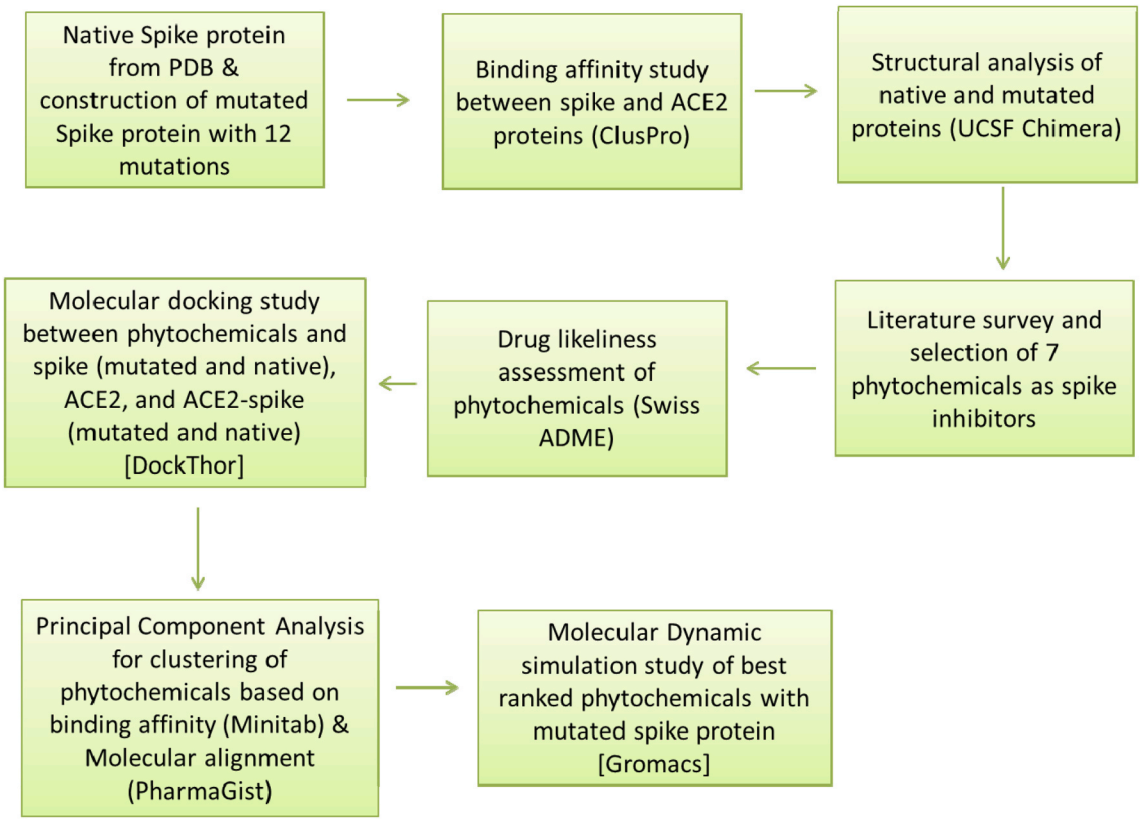

Fig. 1. Flowchart depicting the process of evaluation to study the efficacy of phytochemicals against native and hypothetical mutated spike (S) protein of SARS-CoV-2 and its interaction with hACE2.

components, i.e. uncorrelated variables. Each of the principal components represents the individual dimension of variations from the measured dataset. A PCA consists of multiple components (PCs), while PC1 covers the maximum variations, the second one is orthogonal to the former and covers the following scale of variations and so on [52]. In this work, PCA was performed by Minitab 18 statistical software to understand the correlation among all the variables (binding affinity scores of different phytochemicals docked with proteins, native and mutated S and S + hACE2 complex). Further, visualization of the comparative docking scores was represented by using the heat map tool of MeV 4.9.0 software. In addition, we performed a molecular alignment study of all seven phytochemicals by using PharmaGist (https://bioinfo3d.cs.tau.ac.il/PharmaGist). PharmaGist is an online server for pharmacophore and molecular alignment, which relies on four principles: 'ligand representation, pairwise alignment, multiple alignment and solution clustering and output'. After performing pairwise alignments with the input ligands, the alignment score is generated based on pivot and conformation features. The alignment score is defined as the weighted sum of the matched pivot features, and a default value of 0.3 is assigned for the hydrophobicity feature and 1 for the rest (aromatic, donor/acceptor groups etc) [53]. The entire workflow, including the steps of the *in silico* docking analysis, is summarized in Fig. 1.

3. Results

3.1. Evaluation of drug-like properties

In this study, seven (7) phytochemicals were screened and evaluated for drug-like properties, presented in Supplementary Fig. S1. BOILED-Egg graphical interface showed that except zingiberene, all six compounds could be absorbed through the human gastrointestinal (HIA) pathway, and all the compounds were PGP negative, indicative of superior bioavailability and negating the chance of effluxing. Finally, Table S1 (presented in supplementary information) showed that all the phytochemicals passed through drug likeliness criteria, namely Total Polar Surface Area (TPSA), Lipophilicity, water solubility and Lipinski rules.

3.2. Predicted mutated S protein

Twelve (12) major mutations were clubbed together and incorporated within a single S protein amino acid sequence to form the predicted hypothetical mutated spike protein.The targeted single letter amino acid codes are underlined in the native spike, while the mutated amino acid codes are underlined and represented as **bold letters** in mutated S protein sequence.

3.2.1. Native S protein amino acid sequence

TNLCPFGEVFNATRFASVYAWNRKRISNCVA-
DYSVLYNSASFSTFKCYGVSPTKLNDLCFTNVYADSFVIRGDEVRQIAPGQ
TGKIADYNYKLPDDFTGCVIAWNSNNLDSKVGGNYNY-
LYRLFRKSNLKPFERDISTEIY-
QAGSTPCNGVEGFNCYFPLQSYGFQPTNGVGYQPYRVVVLSFELLHA-
PATVCGPKKSTNLVKNKCVNF.

3.2.2. Mutated S protein amino acid sequence

TNLCPFGEVFNATRFASVYAWNRKRISNCVA-
DYSVLYNSASFSTFKCYG**LSL**TKLNDLCFTNVYADSFVIRGDEVRQIAPGQ
TG**N**IADYNYKLPDDFTGCVIAWNS**K**NLDSKVGGNY-
NYL**F**RLFRKSNLKPFERDISTEIY-
QAG**NIP**CNGV**K**GFNCYFPLQ**P**YGFQPT**Y**GVGYQPYRVVVLS-
FELLH**SPV**TVCGPKK**S**TNLVKNKCVNF

3.3. hACE2-spike/mutated spike interaction

Prodigy prediction showed an increase in the binding affinity of mutated S with the hACE2 protein. While the SARS-CoV-2 spike showed −12.6 kcal mol-^{1} binding energy for interaction with hACE2 protein, the hypothetical mutated spike was found to be −13.2 kcal mol-^{1,} indicating its stronger interaction with hACE2 than the native one. The accumulated mutations changed the predicted S protein's conformation and made it more potent to bind the human ACE2 protein (Fig. 2). Mutated residues (LYS484, ILE478 and ASN477) changed the beta strands to the coil. Similarly, mutations at VAL522, LEU382, SER520 and LEU384 changed beta-strand to the coiled structure. Mutations also changed coiled structure conformations at PRO494, PHE453, ASN417, TYR501 and LYS439.

3.4. Docking interaction between different phytochemicals with proteins

Out of seven phytochemicals studied here, we found that three compounds, namely curcumin, piperine and zingiberene, could strongly bind with native S protein (−7.696, −8.084 and −7.695 kcal mol^{-1}, respectively), compared to the control drug chloroquine (−7.586 kcal mol^{-1}). Along with these three phytochemicals (curcumin: -7.958, piperine: -7.449 and zingiberene: -8.081 kcal mol^{-1} respectively), gingerol and capsaicin (−7.603 and −7.867 kcal mol^{-1}, respectively) were also found to show binding potential with the mutated S protein. It is noteworthy that these compounds even showed greater binding affinity towards the mutated and native S-hACE2 protein complexes, making them ideal candidates for disrupting spike-hACE2 complex (Table 1). The interacting amino acids of spike proteins (native and mutated) with that of curcumin, piperine and the control drug chloroquine are presented in Fig. 3. We have found that, interactions at GLU484 for native S protein and CYS133, TRP163 for hACE2 protein are common for curcumin and chloroquine. Curcumin was found to bind the mutated S through an interaction with an altered amino acid LYS484. Both curcumin and piperine showed stronger binding affinities towards the mutated S-ACE2 complex than chloroquine (−10.568, −10.0 and −9.774 kcal mol^{-1}, respectively). Chloroquine and piperine both had the same interaction at PRO494 (altered from ASP494) of the mutated S-hACE2 complex. LEU452 of spike protein was the common interaction point for curcumin, piperine, and chloroquine in ligand binding with mutated S-hACE2 complex (Fig. 4). Our additional 'hACE2 inhibitor control' GR 127935 hydrochloride also showed comparable hACE2 binding potential (−8.934 kcal mol^{-1}) with curcumin (−8.599 kcal mol^{-1}). For S-hACE2 complexes (native and mutated S), binding affinities of the selected hACE2 inhibitor (−8.300 and −11.537 kcal mol^{-1} for native and mutated S-ACE2 complexes respectively) were comparable with both the phytochemicals namely, curcumin (−8.249 and −10.568 kcal mol^{-1} for native and mutated S-hACE2 complexes respectively) and piperine (−8.362 and -10.000 kcal mol^{-1} for native and mutated S-hACE2 complexes respectively). Therefore, based on the overall docking results of the various targets, curcumin and piperine were selected and further subjected to evaluate the docking stability with spike proteins by the Molecular Dynamic simulation technique. Detailed interaction sites are mentioned in Supplementary Tables S2 and S3. Interaction between GR 127935 hydrochloride and target proteins are shown in the Supplementary Fig. S6.

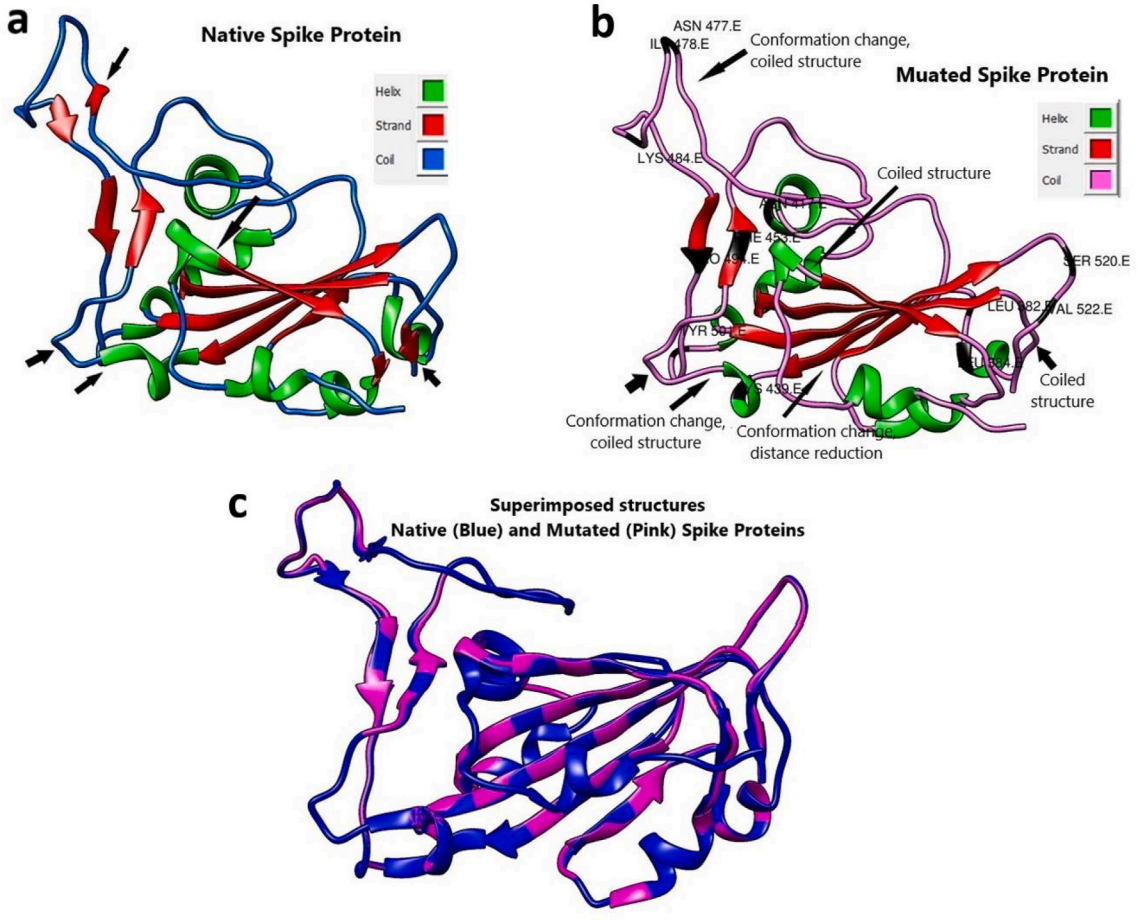

Fig. 2. Structural comparison of native and mutated spike (S) proteins showing conformational changes; (**a**) Native S protein showing helix, strand and coil structures; (**b**) Mutated S protein showing helix, strand and coil structures; (**c**) Superimposed structures of native (blue) and mutated (pink) spike proteins.

Table 1
Result of docking interactions between compounds, spike proteins (S) and S-hACE2 (Angiotensin-converting enzyme 2) protein complex; scores higher than the control, are marked in **bold**.

PubChem id	Compounds	Docking Energy (kcal mol^{-1})				
		Native S	Mutated S	ACE2	ACE2 + Native S	ACE2 + Mutated S
CID_2719	Chloroquine	−7.586	−7.079	−7.757	−8.321	−9.774
CID_107780	GR 127935 hydrochloride	-	-	−8.934	−8.300	−11.537
CID_65036	Allicin	−6.709	−6.68	−6.666	−6.709	−8.133
CID_1548943	Capsaicin	−7.467	**−7.867**	−7.798	−7.927	−9.385
CID_637511	Cinnamaldehyde	−6.696	−7.245	−6.833	−6.672	−8.066
CID_969516	Curcumin	**−7.696**	**−7.958**	**−8.599**	**−8.249**	**−10.568**
CID_442793	Gingerol	−7.049	**−7.603**	−7.434	−7.947	−9.221
CID_638024	Piperine	**−8.084**	**−7.449**	−7.708	**−8.362**	**−10.000**
CID_92776	Zingiberene	**−7.695**	**−8.081**	**−8.069**	−7.555	−7.824

3.5. Docking validation by MD simulation

To understand the overall conformational dynamics and stability of the protein-ligand structures (Phytochemicals-native S and Phytochemicals-mutated S), RMSD (Root Mean Square Deviation) values, relative to the starting position of the backbone of all amino acid residues, were calculated. The average RMSD for curcumin-native S and curcumin-mutated S were found to be 0.32 and 0.38 nm, respectively. Further, average RMSD scores of Piperine-native S and Piperine-mutated S were found to be 0.28 and 0.27 nm. All the values were comparable

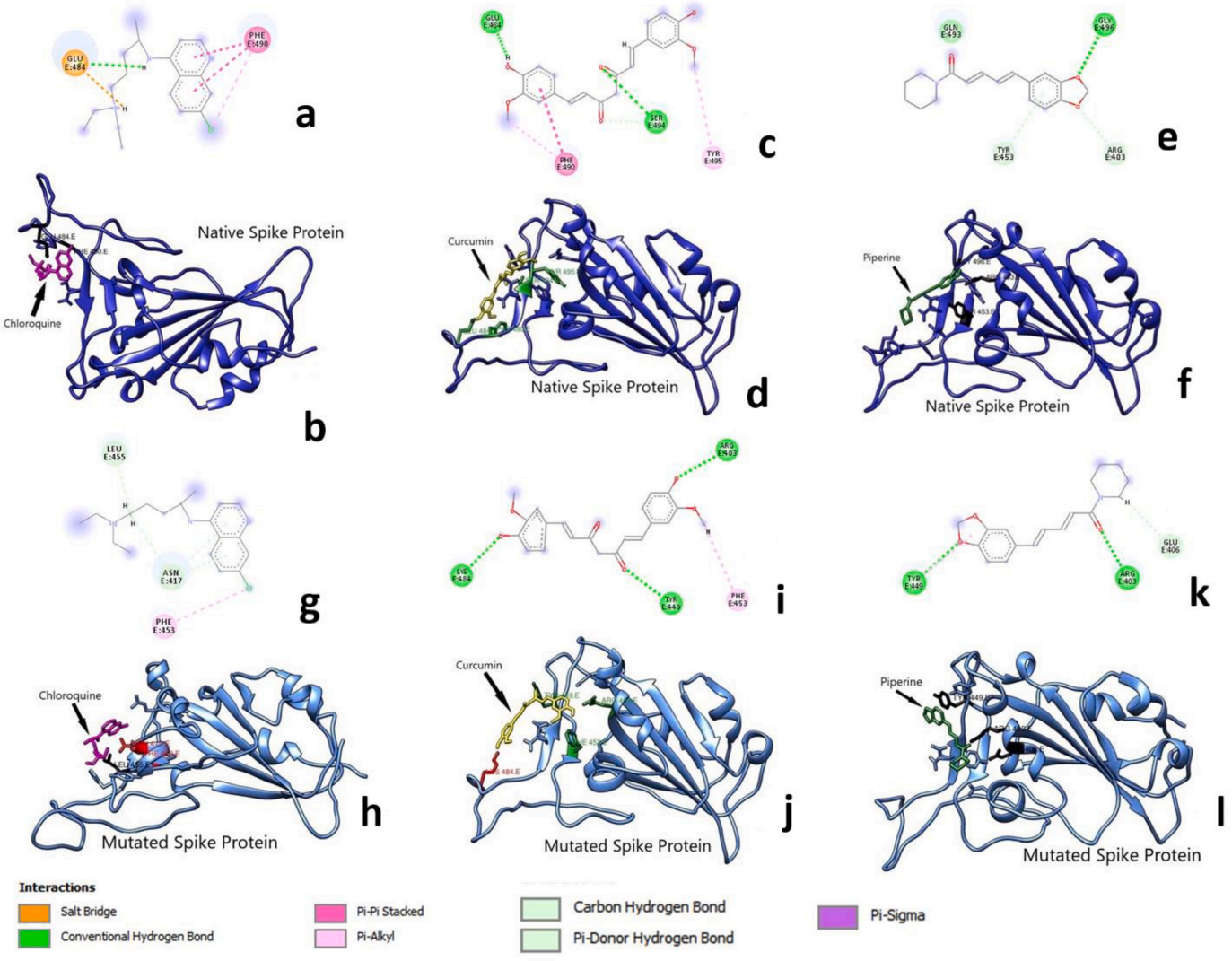

Fig. 3. Interaction of control drug chloroquine and selected phytochemicals (curcumin and piperine) with spike (S) proteins (native and mutated); (**a**) 2D representation and (**b**) representative ribbon structure of chloroquine-native S protein interaction, (**c**) 2D representation and (**d**) representative ribbon structure of curcumin-native S protein interaction, (**e**) 2D representation and (**f**) representative ribbon structure of piperine-native S protein interaction, (**g**) 2D representation and (**h**) representative ribbon structure of chloroquine-mutated S protein interaction, (**i**) 2D representation and (**j**) representative ribbon structure of curcumin-mutated S protein interaction, (**k**) 2D representation and (**l**) representative ribbon structure of piperine-mutated S protein interaction.

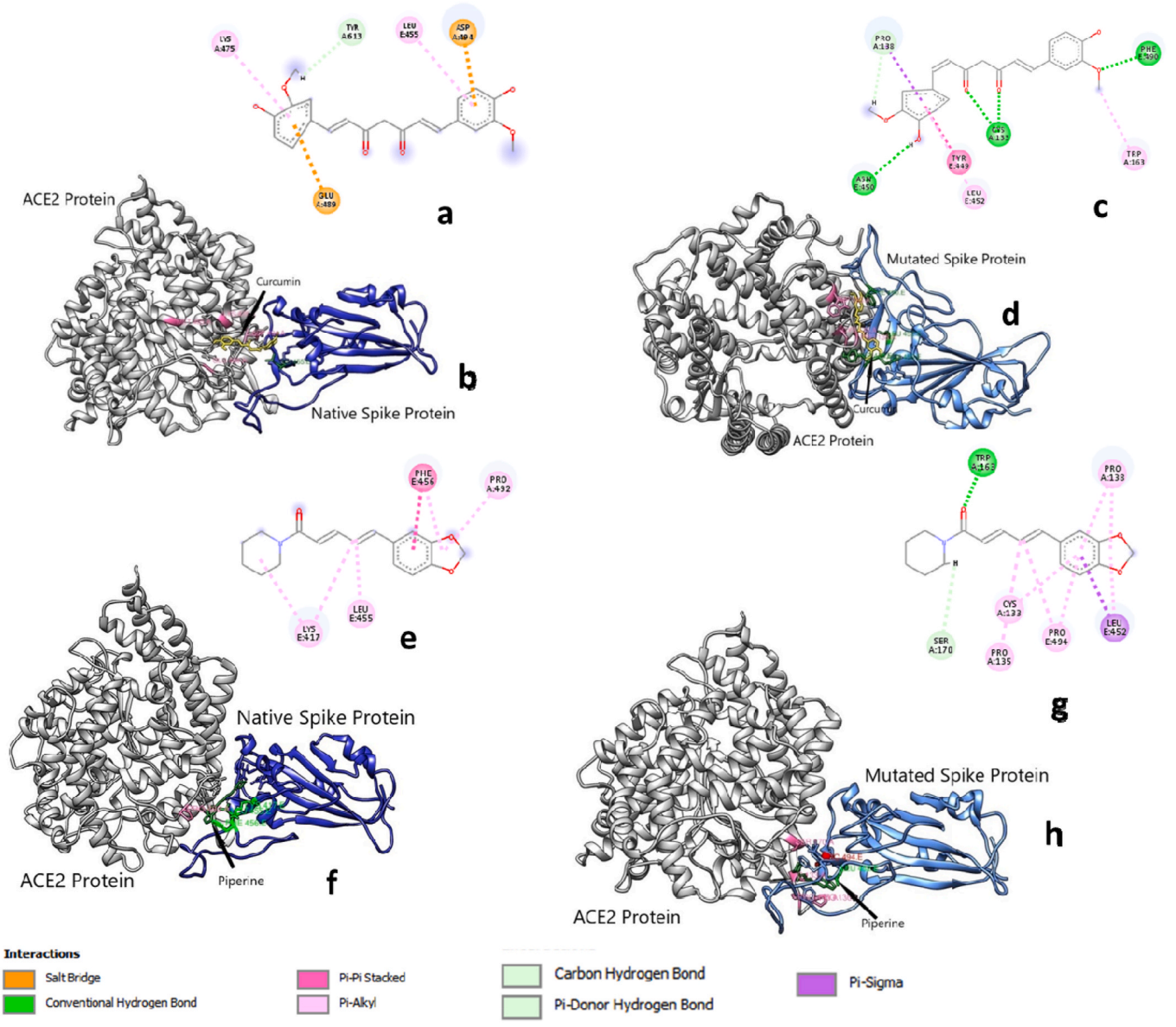

Fig. 4. Representation of selected phytochemicals, hACE2 and Spike (S) protein interactions; (**a**) 2D representation of Curcumin-ACE2-native S Protein &(**b**) Curcumin-ACE2-native SProtein; (**c**) 2D representation of curcumin-ACE2- Mutated S Protein& (**d**) Curcumin-ACE2-Mutated S Protein; (**e**) 2D representation of Piperine-ACE2-Native S Protein& (**f**) Piperine-ACE2-Native S Protein; (**g**) 2D representation of Piperine -ACE2- Mutated S Protein& (**h**) Piperine-ACE2-Mutated S Protein.

and indicative of the stability of ligand-protein interaction in the physiological environment. When curcumin and piperine interactions with native S protein were compared, it was observed that they reached equilibrium after~25 and ~20 ns, respectively and continued to be stable until the simulation ended at 100 ns.

Further, the mutated S- piperine complex remained stable throughout the simulation time, i.e. 100 ns. However, curcumin showed two splits in the simulation trajectory at around 5 and 40 ns, possibly due to the more complex structure than its counterpart. After 40 ns, however, curcumin remained in equilibrium till the end of the simulation, i.e. up to 100 ns (Fig. 5a and b). In native S, curcumin and piperine largely stabilized within the range of ~0.20–0.35 and ~0.20–0.38 nm RMSD, respectively. Whereas, in the case of mutated S, curcumin and piperine stabilized within the range of 0.30–0.40 and ~0.20–0.35 nm, respectively (as presented in the supplementary information, Fig. S2a). Hence, the results from RMSD showed that curcumin and piperine remained positioned at the active sites of the respective proteins with stable interactions with both the proteins, i.e. native and mutated ones.

Dynamic adaptability and compactness of the ligand-protein complexes in the aqueous environment were evaluated by the gyration (Rg) radius, as shown in Fig. 5b and f. Rg values of curcumin and piperine with native and mutated S proteins ranged between ~1.7–1.9 and ~1.7–1.8, respectively. For native S complexes, the significant population of Rg values lie within the close range of ~1.80–1.82 nm, while for mutated ones; the range was ~1.75–1.80 nm (represented in Supplementary Fig. S2b). Thus, the overall results of gyration showed that, protein-ligand complexes had minimum variations in terms of structural compactness, which in turn indicated the stability of the complexes, consistent with the result of RMSD.

Structural stability of the ligand-bound proteins in the aqueous environment was further evaluated by SASA (Solvent-Accessible Surface Area). It was observed that the frequencies of SASA of all the complexes were restricted around 100 nm^2 (Fig. 5c and g) and were entirely in equilibrium throughout the simulation range. All the complexes showed

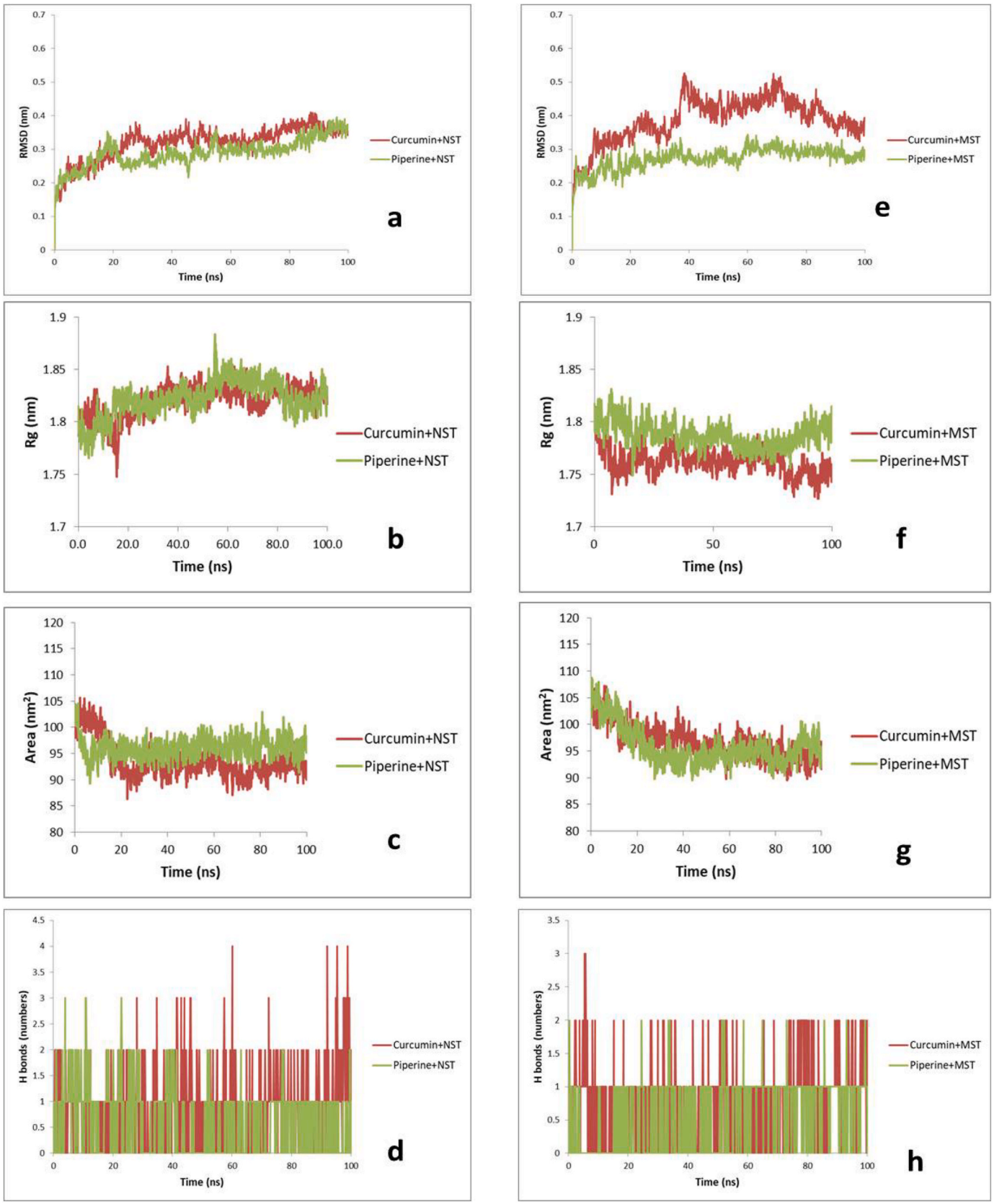

Fig. 5. MD simulation of curcumin and piperine with Native (NST) and Mutated spike proteins (MST); (a)–(e): RMSD line plots for NST and MST, (b)–(f): Radius of gyration (Rg) line plots for NST and MST, (c)–(g): Solvent Accessible Surface Area (SASA) line plots for NST and MST; (d)–(h): Line plots of Ligand-protein H bonds for NST and MST.

stable conformational dynamics for all structures, i.e. native and mutated S protein associations with curcumin and piperine. Hence, the results obtained collectively from all the three parameters, namely RMSD, Rg, and SASA, clearly showed that phytochemical-protein complexes are stable and capable of inhibiting both native and mutated S proteins by binding to their respective active sites.

In addition to the three parameters mentioned above, we also evaluated H-bond formation dynamics between ligands and proteins. For interaction with native spike protein, curcumin and piperine showed a maximum of 4 and 3 H bonds, respectively, with their proteins (Fig. 5d). Curcumin and piperine showed a similar trend for mutated S protein with 3 and 2 H bonds, respectively (Fig. 5h). However, at least 1 H bond was found to be long-lived throughout the simulation of 100 ns for all the complexes (as shown in Supplementary Fig. S2d).

3.6. Statistical analysis, heat map generation and molecular alignment

The heat map (Fig. 6a) showed that curcumin and piperineare more efficient than the control drug to bind with target proteins and form complexes. In the PCA analysis (Fig. 6b), it was observed that the First and Second Components together contributed towards 91.2% variability from the overall data. Hence, as shown in Fig. 6b, the first two components can cover the dataset's maximum variations. We observed four distinct clusters in the PCA. Cluster I was contributed by curcumin, piperine and chloroquine. The remaining compounds were divided into three clusters, as shown in the figure (capsaicin-gingerol; cinammaldehyde-zingiberene and allicin). Although placed in different PCA clusters, capsaicin and gingerol were also placed near curcumin-piperine groups.

We observed structural similarity of these four phytochemicals (capsaicin, gingerol, curcumin and piperine) in the molecular alignment study and the results were presented in details in the supplementary information (Figs. S3 and S4). With the alignment score of 16.668, one hydrophobic, one aromatic and two acceptor features were detected as similar descriptors in these four compounds.

Further, based on the docking results, we performed molecular alignment study with two top phytochemicals, namely curcumin and piperine, along with the control drug chloroquine, (Fig. S5). The study revealed that, one aromatic and two acceptor groups are common pharmacophores in both the phytochemicals. When compared with the docking interaction results of these compounds and spike proteins (native and mutated), these features were found to be the major interacting groups with the amino acid residues (Fig. 7).

4. Discussion

Spike (S) protein, the major protein responsible for entry and pathogenicity of the SARS-CoV-2 virus, is continuously mutating through steady transmission in humans. Several studies have already established that the frequent mutations in S protein led to an increase in the infectivity of the virus through the enhanced binding to human ACE2 protein [54]. Further, it was observed from the literature that the accumulation of various mutations in the spike protein, such as N501Y, S494P, E484K etc caused enhanced affinity of the S protein to the human ACE2 receptor [55,56]. Chen et al. [10] showed increased spike-ACE2 binding energy with high mutation rates in several residues (452, 489, 500, 501, and 505). Therefore, it is evident that accumulating mutations in SARS-CoV-2 spike protein may give rise to variant of concern (VOC) which may show drug resistance and can even evade the vaccine-induced acquired immunity. Phytochemicals are now considered as the safe and effective alternative in treating COVID-19 infection, and various reports showed their potential as anti-COVID 19 agents [57]. Integration of the modern computational biology approach and traditional experimentations significantly expedited the initial screening of natural compounds against SARS-CoV-2 [58,59]. In our present work, we investigated the inhibitory potentials of seven phytochemicals, namely allicin, capsaicin, cinnamaldehyde, curcumin, gingerol, piperine and zingeberene against SARS-CoV-2 mutant spike proteins. While allicin is the principal compound of garlic (*Allium sativum*), capsaicin is commonly sourced from chili pepper (*Capsicum frutescens*). Gingerol and zingiberene, cinnamaldehyde, curcumin and piperine were found in ginger (*Zingiber officinale*), cinnamon (*Cinnamomum verum*), turmeric (*Curcuma longa*) and pepper (*Piper nigrum*) respectively (https://phytochem.nal.usda.gov/). The decoction (known as kadha in Indian Ayurveda system) prepared from these herbs is commonly used against common cold and is suggested to be effective against COVID-19 pathogenesis. Maurya and Sharma [60] had undertaken an *in silico* approach to study the beneficial effect of major phytochemicals present in kadha against,SARS-CoV-2. Further, Gautam and coworkers [61] reported that such herbal decoction possessed significant anti-viral and immunomodulatory properties.

Recently, Jena et al. [57] showed that curcumin and catechin could strongly bind with S protein and S-ACE2 complex; in another preprint, Utomo et al. [20] also reported high binding affinities of curcumin with spike receptor binding domain (RBD) of S protein and ACE2 complex. We also observed a similar binding capacity of curcumin towards RBD and RBD-ACE2 complex, which is in agreement with these findings.

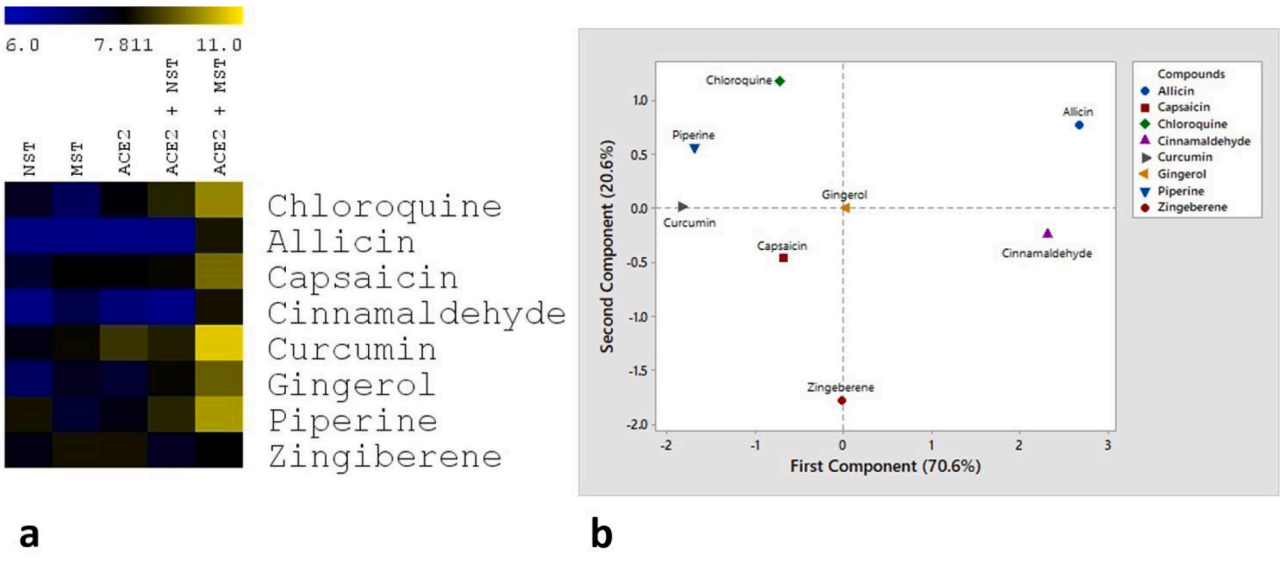

Fig. 6. (a) Heat map of the docking scores as created by MEV 4.9.0; (**b**) Principal Component Analysis of docking scores as generated by Minitab 18.

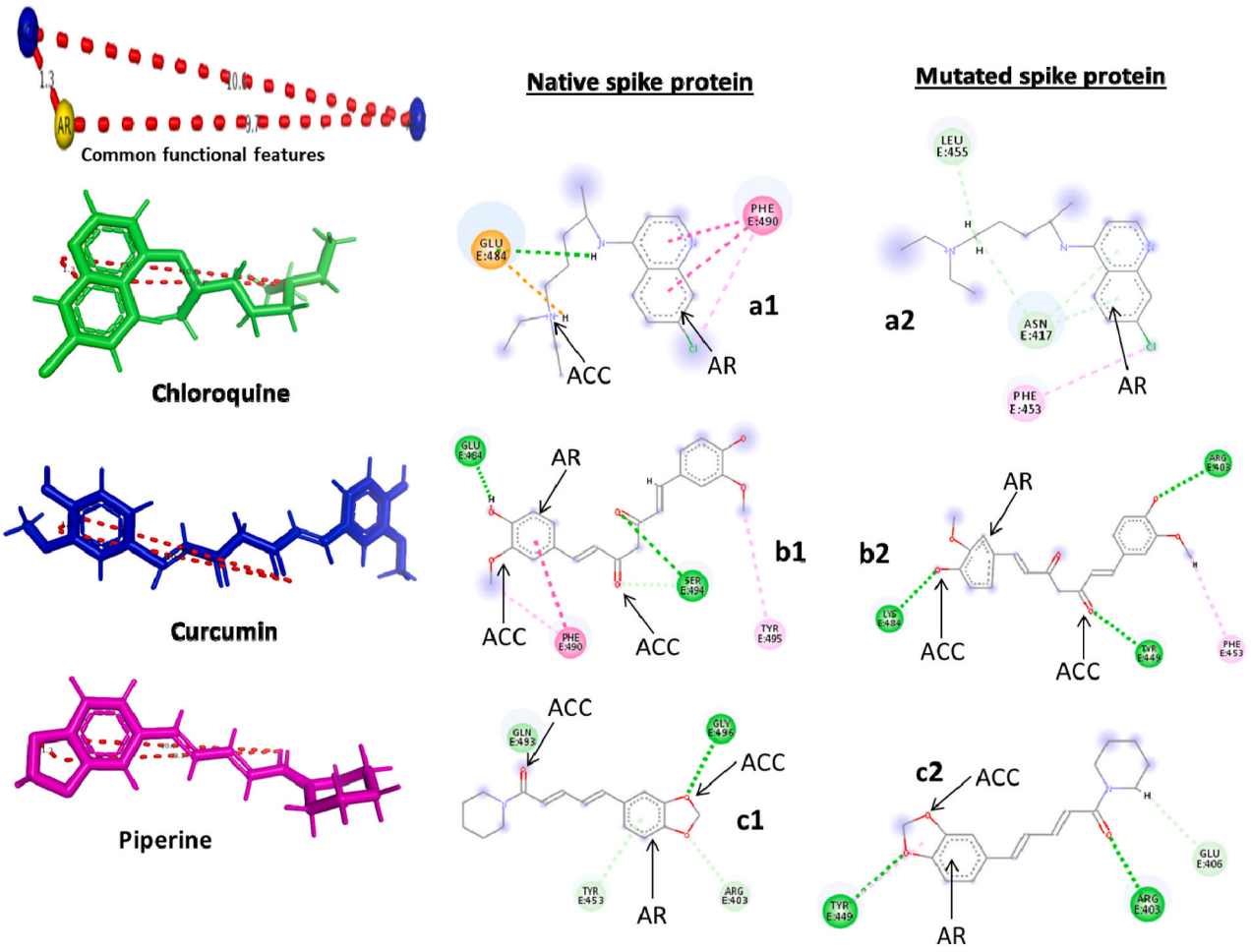

Fig. 7. Phytochemical-spike protein interacting groups and alignment with the common pharmacophores (features) as determined by molecular alignment (PharmaGist); ACC: Acceptor and AR: Aromatic groups; **a1-c1:** Native spike protein-compound interactions (chloroquine, curcumin and piperine respectively); **a2-c2:** Mutated spike protein-compound interactions (chloroquine, curcumin and piperine respectively).

Furthermore, in our study, curcumin showed strong binding potential with our predicted mutated spike protein and mutated S-ACE2 complex. The binding of phytochemical to the S-ACE2 complex was critical as such interaction could alter the stability of the complex and thereby could inhibit the entry of the virus into the host body. Basu et al. [19] showed that the phytochemical hesperidin caused destabilization of S-ACE2 complex in an *in silico* study. Along with curcumin, piperine was also found to have overall efficacy in binding native and spike protein complexes. Piperine was reported to be a powerful antioxidant and anti-inflammatory agent. In a double-blind, randomized, controlled trial with a population size of thirty (30) in Maharashtra, India, Pawar et al. [62] reported the encouraging outcomes (oxygen saturation above 94% on room air and early symptomatic recovery) of oral combination therapy of curcumin and piperine against SARS-CoV-2. A similar study was undertaken in Iran as a randomized, placebo-controlled, double--blind, parallel-arm clinical trial with the age limit < 20 and > 75 years [49]. In our previous study, we reported the anti-viral role of piperine, against Dengue virus [51]. Density functional theory (DFT) analysis may define the activity of compounds based on the calculated band energy gaps. Narrow band energy gap was generally translated into high pharmacological activity of the therapeutic compounds, as indicated by the literature [63]. The HOMO (Highest Occupied Molecular Orbital) and LUMO (Lowest Unoccupied Molecular Orbital) values represent the charge transfer in the chemical reaction [64]. The HOMO and LUMO values of piperine were reported as −5.34 and −1.65 eV, respectively with an energy gap of 3.68 eV [65]. Further, Shahab et al. [66] showed the HOMO and LUMO values of curcumin as −5.55 and −1.97 eV with an energy gap of 3.58 eV. Although we found that the band energy gaps of these two compounds were comparable, curcumin showed slightly higher activity than piperine.

Molecular Dynamic (MD) simulation is a commonly used technique employed by various researchers to evaluate the stability of the protein-ligand complexes in the physiological environment. Pandey et al. [52] showed stability of fisetin, quercetin, and kaempferol with S-ACE2 protein complex of SARS-CoV-2 using MD simulation technique and four assessment parameters, namely RMSD, gyration, SASA and H bond. Furthermore, in another *in silico* study, Bhowmik et al. [53] showed that phytochemical orientin formed a stable complex with SARS-CoV-2 spike protein as revealed by the MD simulation study. Consistent with these studies, the application of MD simulation in our work established the stability of curcumin and piperine with native and mutated Spike proteins and validated the docking results.

The application of statistical tools such as Principal Component Analysis (PCA) is widespread in literature. PCA creates multiple clusters from a given dataset based on their recorded statistical variations. Gad et al. [67] studied the phytochemical composition of different *Pinus* species and classified them by using a PCA tool. Similarly, Mokaya et al. [68] applied the PCA tool to classify the samples based on sampling locations of Royal jelly secreted by honeybees and, it helped authors to understand the geographical influence. In our previous studies on dengue [69] and SARS-CoV-2 viruses [70], we successfully deployed this statistical tool to understand the relation among phytochemicals based

on their docking performances against the viral protein targets. In the present investigation, we identified the structural similarity of curcumin and piperine based on the common features (one hydrophobic, one aromatic and two acceptor groups) by simultaneous applications of PCA and molecular alignment tools. Finally, this study aimed to target multiple point mutations accumulated in the viral spike protein because a single mutation in a protein is primarily non-functional. For example, the effect of the recent dominant spike mutation of D61G is still unknown despite considering various *in vitro* and clinical studies [54]. However, it should be noted that being an RNA virus, COVID-19 mutates very fast and therefore, each day, the international agencies report a large number of mutations. Consequently, it is impossible to accommodate all such mutations in a single scientific study, and this canbe a limitation for any research article, including ours. Nevertheless, it can shed light on a novel finding considering the uniqueness of this study to target mutated spike protein by natural compounds.

5. Conclusion

In the present study, we identified curcumin and piperine (among seven screened phytochemicals) as potential therapeutic entities, which were found to optimally inhibit predicted mutated spike protein (S, with 12 mutations at different points) of SARS-CoV-2, and could disrupt the mutated S-hACE2 complex. These phytochemicals were screened based on the comparison of binding scores with that of the control drug chloroquine. We observed that curcumin and piperine used similar amino acid residue ARG403 to bind with the mutated S protein. Additionally, curcumin interacted with the mutated amino acid residue LYS484 through the H bond to stabilize the binding with the receptor. Piperine and curcumin could inhibit the native S protein and disrupt the subsequent S-hACE2 complex as well. Statistical and molecular alignment studies revealed that these two compounds shared common functional features like H-bond acceptor, hydrophobic and aromatic groups. Finally, curcumin and piperine could stabilize their respective target proteins, as determined by the molecular dynamic simulation.

Declaration of competing interest

Financial segment: This research was not funded by any government or private organization. Authors are from three respective universities that are not going to get/loss financially from the publication. No patent or patent applications were filed, either by the authors or from the respective institutions. Non-Financial segment: Authors are not associated with any organization that has a stake in this research publication. Declaration: Authors declare that, they have no competing interest.

Acknowledgements

Authors duly acknowledge Department of Life Sciences, CHRIST (Deemed to be University); Bangalore; School of Biotechnology, Presidency University, Kolkata; School of Biological and Environmental Sciences, Shoolini University, Solan and Department of Botany, University of Calcutta, Kolkata for providing institutional and administrative supports as and when required. We extend our acknowledgement to Center for Academic & Professional Support, CHRIST (Deemed to be University), Bangalore and Ms. Anindita Das, MA (English) for language correction as a professional English linguist.

Appendix A. Supplementary data

Supplementary data to this article can be found online at https://doi.org/10.1016/j.compbiomed.2021.104818.

Author contributions

A.N. conceived, designed the study & performed the experimentations; Primary data analysis & manuscript draft preparation were done by S.P. Secondary data analysis & finalization of the manuscript were done by R.B. and Critical review & supervision of the work were done by R.K. All authors read and approved the final manuscript.

References

[1] WHO Coronavirus (COVID-19) Dashboard, (n.d.). https://covid19.who.int (accessed April 23, 2021).
[2] D. Kim, J.-Y. Lee, J.-S. Yang, J.W. Kim, V.N. Kim, H. Chang, The architecture of SARS-CoV-2 transcriptome, Cell 181 (2020) 914–921, https://doi.org/10.1016/j.cell.2020.04.011, e10.
[3] P. Zhou, X.-L. Yang, X.-G. Wang, B. Hu, L. Zhang, W. Zhang, H.-R. Si, Y. Zhu, B. Li, C.-L. Huang, H.-D. Chen, J. Chen, Y. Luo, H. Guo, R.-D. Jiang, M.-Q. Liu, Y. Chen, X.-R. Shen, X. Wang, X.-S. Zheng, K. Zhao, Q.-J. Chen, F. Deng, L.-L. Liu, B. Yan, F.-X. Zhan, Y.-Y. Wang, G.-F. Xiao, Z.-L. Shi, A pneumonia outbreak associated with a new coronavirus of probable bat origin, Nature 579 (2020) 270–273, https://doi.org/10.1038/s41586-020-2012-7.
[4] Y. Wan, J. Shang, R. Graham, R.S. Baric, F. Li, Receptor recognition by the novel coronavirus from wuhan: an analysis based on decade-long structural studies of SARS coronavirus, J. Virol. 94 (2020), https://doi.org/10.1128/JVI.00127-20 e00127-20.
[5] H.M. Ashour, W.F. Elkhatib, M.M. Rahman, H.A. Elshabrawy, Insights into the recent 2019 novel coronavirus (SARS-CoV-2) in light of past human coronavirus outbreaks, Pathog. Basel Switz. 9 (2020), https://doi.org/10.3390/pathogens9030186.
[6] M. Uddin, F. Mustafa, T.A. Rizvi, T. Loney, H.A. Suwaidi, A.H.H. Al-Marzouqi, A. K. Eldin, N. Alsabeeha, T.E. Adrian, C. Stefanini, N. Nowotny, A. Alsheikh-Ali, A. C. Senok, SARS-CoV-2/COVID-19: viral genomics, epidemiology, vaccines, and therapeutic interventions, Viruses 12 (2020), https://doi.org/10.3390/v12050526.
[7] A.C. Walls, Y.-J. Park, M.A. Tortorici, A. Wall, A.T. McGuire, D. Veesler, Structure, function, and antigenicity of the SARS-CoV-2 spike glycoprotein, Cell 181 (2020) 281–292, https://doi.org/10.1016/j.cell.2020.02.058, e6.
[8] N. Nao, J. Yamagishi, H. Miyamoto, M. Igarashi, R. Manzoor, A. Ohnuma, Y. Tsuda, W. Furuyama, A. Shigeno, M. Kajihara, N. Kishida, R. Yoshida, A. Takada, Genetic predisposition to acquire a polybasic cleavage site for highly pathogenic avian influenza virus hemagglutinin, mBio 8 (2017), https://doi.org/10.1128/mBio.02298-16.
[9] I. Bagdonaite, H.H. Wandall, Global aspects of viral glycosylation, Glycobiology 28 (2018) 443–467, https://doi.org/10.1093/glycob/cwy021.
[10] J. Chen, R. Wang, M. Wang, G.-W. Wei, Mutations strengthened SARS-CoV-2 infectivity, J. Mol. Biol. 432 (2020) 5212–5226, https://doi.org/10.1016/j.jmb.2020.07.009.
[11] F. Ali, A. Kasry, M. Amin, The new SARS-CoV-2 strain shows a stronger binding affinity to ACE2 due to N501Y mutant, Med. Drug Discov. 10 (2021), 100086, https://doi.org/10.1016/j.medidd.2021.100086.
[12] F. Naveca, COVID-19 Epidemic in the Brazilian State of Amazonas Was Driven by Long-Term Persistence of Endemic SARS-CoV-2 Lineages and the Recent Emergence of the New Variant of Concern P., (n.d.) 21.
[13] N.R. Faria, T.A. Mellan, C. Whittaker, I.M. Claro, D. da S. Candido, S. Mishra, M.A. E. Crispim, F.C. Sales, I. Hawryluk, J.T. McCrone, R.J.G. Hulswit, L.A.M. Franco, M.S. Ramundo, J.G. de Jesus, P.S. Andrade, T.M. Coletti, G.M. Ferreira, C.A. M. Silva, E.R. Manuli, R.H.M. Pereira, P.S. Peixoto, M.U. Kraemer, N. Gaburo, C. da C. Camilo, H. Hoeltgebaum, W.M. Souza, E.C. Rocha, L.M. de Souza, M.C. de Pinho, L.J.T. Araujo, F.S.V. Malta, A.B. de Lima, J. do P. Silva, D.A.G. Zauli, A.C. de S. Ferreira, R.P. Schnekenberg, D.J. Laydon, P.G.T. Walker, H.M. Schlüter, A.L. P. dos Santos, M.S. Vidal, V.S. Del Caro, R.M.F. Filho, H.M. dos Santos, R.S. Aguiar, J.L.P. Modena, B. Nelson, J.A. Hay, M. Monod, X. Miscouridou, H. Coupland, R. Sonabend, M. Vollmer, A. Gandy, M.A. Suchard, T.A. Bowden, S.L.K. Pond, C.-H. Wu, O. Ratmann, N.M. Ferguson, C. Dye, N.J. Loman, P. Lemey, A. Rambaut, N. A. Fraiji, , M. do P.S.S. Carvalho, O.G. Pybus, S. Flaxman, S. Bhatt, E.C. Sabino, Genomics and Epidemiology of a Novel SARS-CoV-2 Lineage in Manaus, Brazil, MedRxiv, 2021, https://doi.org/10.1101/2021.02.26.21252554.
[14] G. Nelson, O. Buzko, P. Spilman, K. Niazi, S. Rabizadeh, P. Soon-Shiong, Molecular dynamic simulation reveals E484K mutation enhances spike RBD-ACE2 affinity and the combination of E484K, K417N and N501Y mutations (501Y.V2 variant) induces conformational change greater than N501Y mutant alone, potentially resulting in an escape mutant, BioRxiv (2021), https://doi.org/10.1101/2021.01.13.426558, 2021.01.13.426558.
[15] J. Koshy, Coronavirus | Indian 'double Mutant' Strain Named B.1.617, The Hindu, 2021. https://www.thehindu.com/news/national/indian-double-mutant-strain-named-b1617/article34274663.ece. (Accessed 23 April 2021).
[16] M. Scudellari, How the coronavirus infects cells — and why Delta is so dangerous, Nature 595 (2021) 640–644, https://doi.org/10.1038/d41586-021-02039-y.
[17] J. Khateeb, Y. Li, H. Zhang, Emerging SARS-CoV-2 variants of concern and potential intervention approaches, Crit. Care 25 (2021) 244, https://doi.org/10.1186/s13054-021-03662-x.
[18] Q. Li, J. Wu, J. Nie, L. Zhang, H. Hao, S. Liu, C. Zhao, Q. Zhang, H. Liu, L. Nie, H. Qin, M. Wang, Q. Lu, X. Li, Q. Sun, J. Liu, L. Zhang, X. Li, W. Huang, Y. Wang, The impact of mutations in SARS-CoV-2 spike on viral infectivity and antigenicity, Cell 182 (2020) 1284, https://doi.org/10.1016/j.cell.2020.07.012.
[19] C.K. Wibmer, F. Ayres, T. Hermanus, M. Madzivhandila, P. Kgagudi, B. Oosthuysen, B.E. Lambson, T. de Oliveira, M. Vermeulen, K. van der Berg,

T. Rossouw, M. Boswell, V. Ueckermann, S. Meiring, A. von Gottberg, C. Cohen, L. Morris, J.N. Bhiman, P.L. Moore, SARS-CoV-2 501Y.V2 escapes neutralization by South African COVID-19 donor plasma, Nat. Med. 27 (2021) 622–625, https://doi.org/10.1038/s41591-021-01285-x.

[20] S. Satarker, T. Ahuja, M. Banerjee, , V.B. E, S. Dogra, T. Agarwal, M. Nampoothiri, Hydroxychloroquine in COVID-19: potential mechanism of action against SARS-CoV-2, Curr. Pharmacol. Rep. 6 (2020) 203–211, https://doi.org/10.1007/s40495-020-00231-8.

[21] M. Mauthe, I. Orhon, C. Rocchi, X. Zhou, M. Luhr, K.-J. Hijlkema, R.P. Coppes, N. Engedal, M. Mari, F. Reggiori, Chloroquine inhibits autophagic flux by decreasing autophagosome-lysosome fusion, Autophagy 14 (2018) 1435–1455, https://doi.org/10.1080/15548627.2018.1474314.

[22] M. Gendrot, J. Andreani, M. Boxberger, P. Jardot, I. Fonta, M. Le Bideau, I. Duflot, J. Mosnier, C. Rolland, H. Bogreau, S. Hutter, B. La Scola, B. Pradines, Antimalarial drugs inhibit the replication of SARS-CoV-2: an in vitro evaluation, Trav. Med. Infect. Dis. 37 (2020), 101873, https://doi.org/10.1016/j.tmaid.2020.101873.

[23] A. Basu, A. Sarkar, U. Maulik, Molecular docking study of potential phytochemicals and their effects on the complex of SARS-CoV2 spike protein and human ACE2, Sci. Rep. 10 (2020), 17699, https://doi.org/10.1038/s41598-020-74715-4.

[24] R.Y. Utomo, M. Ikawati, E. Meiyanto, Revealing the Potency of Citrus and Galangal Constituents to Halt SARS-CoV-2 Infection, 2020, https://doi.org/10.20944/preprints202003.0214.v1.

[25] T.-Y. Chen, D.-Y. Chen, H.-W. Wen, J.-L. Ou, S.-S. Chiou, J.-M. Chen, M.-L. Wong, W.-L. Hsu, Inhibition of enveloped viruses infectivity by curcumin, PloS One 8 (2013), e62482, https://doi.org/10.1371/journal.pone.0062482.

[26] A. Nag, A. Mukherjee, In silico docking analysis of Janus kinase enzymes and phytochemicals, J. Chem. Pharmaceut. Res. 6 (2014). https://www.jocpr.com/abstract/in-silico-docking-analysis-of-janus-kinase-enzymes-and-phytochemicals-6131.html. (Accessed 23 March 2021).

[27] F. Zahedipour, S.A. Hosseini, T. Sathyapalan, M. Majeed, T. Jamialahmadi, K. Al-Rasadi, M. Banach, A. Sahebkar, Potential effects of curcumin in the treatment of COVID-19 infection, Phytother. Res. PTR. 34 (2020) 2911–2920, https://doi.org/10.1002/ptr.6738.

[28] D. Ting, N. Dong, L. Fang, J. Lu, J. Bi, S. Xiao, H. Han, Multisite inhibitors for enteric coronavirus: antiviral cationic carbon dots based on curcumin, ACS Appl. Nano Mater. 1 (2018) 5451–5459, https://doi.org/10.1021/acsanm.8b00779.

[29] S. Khaerunnisa, H. Kurniawan, R. Awaluddin, S. Suhartati, S. Soetjipto, Potential Inhibitor of COVID-19 Main Protease (Mpro) from Several Medicinal Plant Compounds by Molecular Docking Study, 2020, https://doi.org/10.20944/preprints202003.0226.v1.

[30] K. Vaibhav, P. Shrivastava, H. Javed, A. Khan, M.E. Ahmed, R. Tabassum, M. M. Khan, G. Khuwaja, F. Islam, M.S. Siddiqui, M.M. Safhi, F. Islam, Piperine suppresses cerebral ischemia-reperfusion-induced inflammation through the repression of COX-2, NOS-2, and NF-κB in middle cerebral artery occlusion rat model, Mol. Cell. Biochem. 367 (2012) 73–84, https://doi.org/10.1007/s11010-012-1321-z.

[31] W.L. DeLano, The PyMOL Molecular Graphics System, 2002. http://www. pymol.org.

[32] G. Ribaudo, P. Coghi, L.J. Yang, J.P.L. Ng, A. Mastinu, M. Memo, V.K.W. Wong, A. Gianoncelli, Computational and experimental insights on the interaction of artemisinin, dihydroartemisinin and chloroquine with SARS-CoV-2 spike protein receptor-binding domain (RBD), Nat. Prod. Res. (2021) 1–6, https://doi.org/10.1080/14786419.2021.1925894.

[33] N. Wang, S. Han, R. Liu, L. Meng, H. He, Y. Zhang, C. Wang, Y. Lv, J. Wang, X. Li, Y. Ding, J. Fu, Y. Hou, W. Lu, W. Ma, Y. Zhan, B. Dai, J. Zhang, X. Pan, S. Hu, J. Gao, Q. Jia, L. Zhang, S. Ge, S. Wang, P. Liang, T. Hu, J. Lu, X. Wang, H. Zhou, W. Ta, Y. Wang, S. Lu, L. He, Chloroquine and hydroxychloroquine as ACE2 blockers to inhibit viropexis of 2019-nCoV Spike pseudotyped virus, Phytomedicine 79 (2020), 153333, https://doi.org/10.1016/j.phymed.2020.153333.

[34] T.R. Machado, M.M.J. Ribeiro, A.C.R. Sodero, T.F.S. Domingos, R. Rapozo, D.C. de Paula, A.S. Domingos, C.R. Rodrigues, L.M. Cabral, A.M.T. de Souza, B. de A. Abrahim-Vieira, Evaluation of chloroquine and hydroxychloroquine as ACE-2 inhibitors by in silico approaches: cardiac arrhythmia cause? J. Mol. Struct. 1244 (2021), 130946 https://doi.org/10.1016/j.molstruc.2021.130946.

[35] S. Choudhary, Y.S. Malik, S. Tomar, Identification of SARS-CoV-2 cell entry inhibitors by drug repurposing using in silico structure-based virtual screening approach, Front. Immunol. (2020), https://doi.org/10.3389/fimmu.2020.01664, 0.

[36] A.K. Rappe, C.J. Casewit, K.S. Colwell, W.A. Goddard, W.M. Skiff, UFF, a full periodic table force field for molecular mechanics and molecular dynamics simulations, J. Am. Chem. Soc. 114 (1992) 10024–10035, https://doi.org/10.1021/ja00051a040.

[37] A. Daina, O. Michielin, V. Zoete, SwissADME: a free web tool to evaluate pharmacokinetics, drug-likeness and medicinal chemistry friendliness of small molecules, Sci. Rep. 7 (2017), 42717, https://doi.org/10.1038/srep42717.

[38] A. Daina, V. Zoete, A BOILED-egg to predict gastrointestinal absorption and brain penetration of small molecules, ChemMedChem 11 (2016) 1117–1121, https://doi.org/10.1002/cmdc.201600182.

[39] D. Kozakov, D.R. Hall, B. Xia, K.A. Porter, D. Padhorny, C. Yueh, D. Beglov, S. Vajda, The ClusPro web server for protein–protein docking, Nat. Protoc. 12 (2017) 255–278, https://doi.org/10.1038/nprot.2016.169.

[40] J.K.A. Kamal, S.A. Benchaar, K. Takamoto, E. Reisler, M.R. Chance, Three-dimensional structure of cofilin bound to monomeric actin derived by structural mass spectrometry data, Proc. Natl. Acad. Sci. U.S.A. 104 (2007) 7910–7915, https://doi.org/10.1073/pnas.0611283104.

[41] J.K.A. Kamal, M.R. Chance, Modeling of protein binary complexes using structural mass spectrometry data, Protein Sci. Publ. Protein Soc. 17 (2008) 79–94, https://doi.org/10.1110/ps.073071808.

[42] D. Padhorny, K.A. Porter, M. Ignatov, A. Alekseenko, D. Beglov, S. Kotelnikov, R. Ashizawa, I. Desta, N. Alam, Z. Sun, E. Brini, K. Dill, O. Schueler-Furman, S. Vajda, D. Kozakov, ClusPro in rounds 38 to 45 of CAPRI: toward combining template-based methods with free docking, Proteins Struct. Funct. Bioinforma. 88 (2020) 1082–1090, https://doi.org/10.1002/prot.25887.

[43] L.C. Xue, J.P. Rodrigues, P.L. Kastritis, A.M. Bonvin, A. Vangone, PRODIGY: a web server for predicting the binding affinity of protein–protein complexes, Bioinformatics 32 (2016) 3676–3678, https://doi.org/10.1093/bioinformatics/btw514.

[44] C.S. de Magalhães, D.M. Almeida, H.J.C. Barbosa, L.E. Dardenne, A dynamic niching genetic algorithm strategy for docking highly flexible ligands, Inf. Sci. 289 (2014) 206–224, https://doi.org/10.1016/j.ins.2014.08.002.

[45] E.F. Pettersen, T.D. Goddard, C.C. Huang, G.S. Couch, D.M. Greenblatt, E.C. Meng, T.E. Ferrin, UCSF Chimera–a visualization system for exploratory research and analysis, J. Comput. Chem. 25 (2004) 1605–1612, https://doi.org/10.1002/jcc.20084.

[46] C. Kutzner, S. Páll, M. Fechner, A. Esztermann, B.L. de Groot, H. Grubmüller, More bang for your buck: improved use of GPU nodes for GROMACS 2018, J. Comput. Chem. 40 (2019) 2418–2431, https://doi.org/10.1002/jcc.26011.

[47] L. Pol-Fachin, C.L. Fernandes, H. Verli, GROMOS96 43a1 performance on the characterization of glycoprotein conformational ensembles through molecular dynamics simulations, Carbohydr. Res. 344 (2009) 491–500, https://doi.org/10.1016/j.carres.2008.12.025.

[48] A.W. Schüttelkopf, D.M.F. van Aalten, PRODRG: a tool for high-throughput crystallography of protein-ligand complexes, Acta Crystallogr. D Biol. Crystallogr. 60 (2004) 1355–1363, https://doi.org/10.1107/S0907444904011679.

[49] J. Huang, S. Rauscher, G. Nawrocki, T. Ran, M. Feig, B.L. de Groot, H. Grubmüller, A.D. MacKerell, CHARMM36m: an improved force field for folded and intrinsically disordered proteins, Nat. Methods 14 (2017) 71–73, https://doi.org/10.1038/nmeth.4067.

[50] G. Bussi, D. Donadio, M. Parrinello, Canonical sampling through velocity rescaling, J. Chem. Phys. 126 (2007), 014101, https://doi.org/10.1063/1.2408420.

[51] M. Parrinello, A. Rahman, Crystal structure and pair potentials: a molecular-dynamics study, Phys. Rev. Lett. 45 (1980) 1196–1199, https://doi.org/10.1103/PhysRevLett.45.1196.

[52] I.T. Jolliffe, J. Cadima, Principal component analysis: a review and recent developments, Philos. Trans. R. Soc. Math. Phys. Eng. Sci. 374 (2016), 20150202, https://doi.org/10.1098/rsta.2015.0202.

[53] D. Schneidman-Duhovny, O. Dror, Y. Inbar, R. Nussinov, H.J. Wolfson, PharmaGist: a webserver for ligand-based pharmacophore detection, Nucleic Acids Res. 36 (2008) W223–W228, https://doi.org/10.1093/nar/gkn187.

[54] S. Ozono, Y. Zhang, H. Ode, K. Sano, T.S. Tan, K. Imai, K. Miyoshi, S. Kishigami, T. Ueno, Y. Iwatani, T. Suzuki, K. Tokunaga, SARS-CoV-2 D614G spike mutation increases entry efficiency with enhanced ACE2-binding affinity, Nat. Commun. 12 (2021) 848, https://doi.org/10.1038/s41467-021-21118-2.

[55] S. Chakraborty, Evolutionary and structural analysis elucidates mutations on SARS-CoV2 spike protein with altered human ACE2 binding affinity, Biochem. Biophys. Res. Commun. 534 (2021) 374–380, https://doi.org/10.1016/j.bbrc.2020.11.075.

[56] P.A.G. Ferrareze, V.B. Franceschi, A. de M. Mayer, G.D. Caldana, R.A. Zimerman, C.E. Thompson, E484K as an innovative phylogenetic event for viral evolution: genomic analysis of the E484K spike mutation in SARS-CoV-2 lineages from Brazil, Infect. Genet. Evol. 93 (2021), 104941, https://doi.org/10.1016/j.meegid.2021.104941.

[57] A.B. Jena, N. Kanungo, V. Nayak, G.B.N. Chainy, J. Dandapat, Catechin and curcumin interact with S protein of SARS-CoV2 and ACE2 of human cell membrane: insights from computational studies, Sci. Rep. 11 (2021) 2043, https://doi.org/10.1038/s41598-021-81462-7.

[58] R. Islam, M.R. Parves, A.S. Paul, N. Uddin, M.S. Rahman, A.A. Mamun, M. N. Hossain, M.A. Ali, M.A. Halim, A molecular modeling approach to identify effective antiviral phytochemicals against the main protease of SARS-CoV-2, J. Biomol. Struct. Dyn. 39 (2021) 3213–3224, https://doi.org/10.1080/07391102.2020.1761883.

[59] S. Kumar, P. Kashyap, S. Chowdhury, S. Kumar, A. Panwar, A. Kumar, Identification of phytochemicals as potential therapeutic agents that binds to Nsp15 protein target of coronavirus (SARS-CoV-2) that are capable of inhibiting virus replication, Phytomedicine Int. J. Phytother. Phytopharm. 85 (2021), 153317, https://doi.org/10.1016/j.phymed.2020.153317.

[60] D.K. Maurya, D. Sharma, Evaluation of traditional ayurvedic Kadha for prevention and management of the novel Coronavirus (SARS-CoV-2) using in silico approach, J. Biomol. Struct. Dyn. (2020) 1–16, https://doi.org/10.1080/07391102.2020.1852119, 0.

[61] S. Gautam, A. Gautam, S. Chhetri, U. Bhattarai, Immunity against COVID-19: potential role of ayush kwath, J. Ayurveda Integr. Med. (2020), https://doi.org/10.1016/j.jaim.2020.08.003.

[62] K.S. Pawar, R.N. Mastud, S.K. Pawar, S.S. Pawar, R.R. Bhoite, R.R. Bhoite, M. V. Kulkarni, A.R. Deshpande, Oral curcumin with piperine as adjuvant therapy for the treatment of COVID-19: a randomized clinical trial, Front. Pharmacol. 12 (2021), 669362, https://doi.org/10.3389/fphar.2021.669362.

[63] A. Majeed, W. Hussain, F. Yasmin, A. Akhtar, N. Rasool, Virtual screening of phytochemicals by targeting HR1 domain of SARS-CoV-2 S protein: molecular docking, molecular dynamics simulations, and DFT studies, BioMed Res. Int. 2021 (2021), 6661191, https://doi.org/10.1155/2021/6661191.

[64] N. Rasool, W. Husssain, Y.D. Khan, Revelation of enzyme activity of mutant pyrazinamidases from Mycobacterium tuberculosis upon binding with various metals using quantum mechanical approach, Comput. Biol. Chem. 83 (2019), 107108, https://doi.org/10.1016/j.compbiolchem.2019.107108.

[65] C.P.O. Aguiar, D.C.F. Lopes, R.S. Borges, Influence of piperidine ring on stability and reactivity of piperine, Chem. Data Collect. 17–18 (2018) 138–142, https://doi.org/10.1016/j.cdc.2018.08.010.

[66] S. Shahab, M. Sheikhi, M. Khaleghian, I. Balakhanava, F. Azarakhshi, DFT study of physisorption effect of the curcumin on CNT(8,0-6) nanotube for biological applications, chin, J. Struct. Chem. 38 (2019) 37–52.

[67] H. Gad, E. Al-Sayed, I. Ayoub, Phytochemical discrimination of Pinus species based on GC–MS and ATR-IR analyses and their impact on Helicobacter pylori, Phytochem. Anal.. n/a (n.d.). https://doi.org/10.1002/pca.3028.

[68] H.O. Mokaya, L.K. Njeru, H.M.G. Lattorff, African honeybee royal jelly: phytochemical contents, free radical scavenging activity, and physicochemical properties, Food Biosci 37 (2020), 100733, https://doi.org/10.1016/j.fbio.2020.100733.

[69] A. Nag, R.R. Chowdhury, Piperine, an alkaloid of black pepper seeds can effectively inhibit the antiviral enzymes of Dengue and Ebola viruses, an in silico molecular docking study, VirusDisease 31 (2020) 308–315, https://doi.org/10.1007/s13337-020-00619-6.

[70] A. Nag, R. Banerjee, R.R. Chowdhury, C. Krishnapura Venkatesh, Phytochemicals as potential drug candidates for targeting SARS CoV 2 proteins, an in silico study, Virusdisease (2021) 1–10, https://doi.org/10.1007/s13337-021-00654-x.